Structure Sensitivity of Methanol Electrooxidation Pathways on Platinum: An On-Line Electrochemical Mass Spectrometry Study

Tom H. M. Housmans,* Ad H. Wonders, and Marc T. M. Koper

Schuit Institute of Catalysis, Laboratory of Inorganic Chemistry and Catalysis, Eindhoven University of Technology, 5600 MB Eindhoven, The Netherlands

Received: October 18, 2005; In Final Form: March 23, 2006

By monitoring the mass fractions of CO_2 (*m*/*z* 44) and methylformate (*m*/*z* 60, formed from $CH_3OH + HCOOH$) with on-line electrochemical mass spectrometry (OLEMS), the selectivity and structure sensitivity of the methanol oxidation pathways were investigated on the basal planes—Pt(111), Pt(110), and Pt(100)—and the stepped Pt electrodes—Pt(554) and Pt(553)—in sulfuric and perchloric acid electrolytes. The maximum reactivity of the MeOH oxidation reaction on Pt(111), Pt(110), and Pt(100) increases in the order Pt(111) < Pt(110) < Pt(100). Mass spectrometry results indicate that the direct oxidation pathway through soluble intermediates plays a pronounced role on Pt(110) and Pt(111), while, on Pt(100), the indirect pathway through adsorbed carbon monoxide is predominant. In 0.5 M H_2SO_4, introducing steps in the (111) plane increases the total reaction rate, while the relative importance of the direct pathway decreases considerably. In 0.5 M $HClO_4$, however, introducing steps increases both the total reaction rate and the selectivity toward the direct oxidation pathway. Anion (sulfate) adsorption on (111) leads to a more prominent role of the direct pathway, but, on all the other surfaces, (bi)sulfate seems to block the formation of soluble intermediates. For both electrolytes, increasing the step density results in more methylformate being formed relative to the amount of CO_2 detected, indicating that the [110] steps themselves catalyze the direct oxidation pathway. A detailed reaction scheme for the methanol oxidation mechanism is suggested based on the literature and the results obtained here.

1. Introduction

Knowledge of the methanol oxidation reaction mechanism on platinum electrodes is of pivotal importance to the development of a low-temperature direct methanol fuel cell (DMFC) and has, therefore, gained continued interest over the past decades.[1,2] In order for these fuel cells to be economically viable, the turnover rate for complete oxidation of methanol must be higher than 0.1 s^{-1} between 0.2 and 0.4 V versus the reversible hydrogen electrode (RHE).[3] However, at these low potentials, the oxidation is incomplete, and poisoning species, including carbon monoxide[1,4−7] and other carbonaceous species (assumed to be HCO or COH),[8−12] are formed during the decomposition of methanol.

One of the main mechanistic issues, which seems to have been resolved recently, is whether the adsorbed carbon monoxide (CO_{ads}) formed during the oxidation of methanol is an intermediate in a serial pathway mechanism or a byproduct in a parallel reaction mechanism. Analyzing oxidation currents and CO coverages, the groups of Wieckowski[13−15] and Stuve[4,16,17] independently showed that the oxidation of methanol can occur at potentials at which adsorbed CO is stable on the surface. These findings were disputed by Vielstich et al., who, on the basis of differential electrochemical mass spectrometry (DEMS), claimed that CO_2 can only be formed at potentials corresponding to the CO oxidation potential.[18] However, as was pointed out by Wang et al., these studies did not take into account the possible formation of soluble side products such as formic acid and formaldehyde.[19−21] From calculations of the current efficiencies recorded on polycrystalline Pt, which, under certain circumstances, are considerably less than 100%, they concluded that a parallel pathway involving incomplete methanol oxidation must indeed exist.

Thus, from a fuel cell perspective, the study of the individual reaction steps in the overall methanol oxidation scheme has been of great interest. On the basis of the Tafel slope obtained from an analysis of the instantaneous methanol oxidation current and an isotope effect analysis, Herrero et al. concluded that the rate-determining step of the methanol adsorption on Pt(110) and Pt(111) is

$$CH_3OH_{sol} \xrightarrow{rds} CH_2OH_{ads} + H^+ + e^- \quad (1)$$

whereas, on Pt(100), it is[13,14]

$$CH_3OH_{sol} \rightarrow CH_2OH_{ads} + H^+ + e^- \quad (2)$$

$$CH_2OH_{ads} \xrightarrow{rds} CHOH_{ads} + H^+ + e^- \quad (3)$$

This mechanism is to be contrasted with the methanol decomposition on platinum in ultrahigh vacuum (UHV), which involves the formation of methoxy (CH_3O) rather than C−H bond breaking. In a previous paper,[22] we reported that the methanol decomposition reaction to form CO, and possibly also soluble intermediates, is structure sensitive and that both the overall rate and the self-poisoning rate increase with the step density. The decomposition of methanol to form CO_{ads} is often identified with the indirect pathway, while the reaction via soluble intermediates is often referred to as the direct pathway. The platinum-catalyzed electrooxidation of CO to CO_2 has been extensively researched by numerous groups.[23−26] On stepped

* Corresponding author. Tel: +31-40-247-4916; fax: +31-40-2455054; e-mail: T.H.M.Housmans@tue.nl.

10.1021/jp055949s CCC: $33.50
Published on Web 04/29/2006

single-crystal electrodes, the oxidation of CO_{ads} was found to occur primarily at step sites.[26−29] In a recent paper by the Wieckowski and Neurock groups, the dual-path mechanism for methanol decomposition on well-defined low Miller index platinum single-crystal electrodes was investigated at potentials where surface-adsorbed CO is stable, using a combination of chronoamperometry, fast scan cyclic voltammetry, and theoretical methods.[30] They concluded that, at potentials between 0.2 and 0.5 V versus RHE, the dual pathway producing products other than adsorbed CO is active on Pt(111) and Pt(110) above 0.35 V versus RHE, whereas, on Pt(100) in the entire potential region under investigation, only complete dehydrogenation of methanol to CO_{ads} occurs, thus signifying the significant structure sensitivity of the dual-path mechanism.

On the basis of ab initio density functional theory (DFT) calculations, they also suggested that a dual dehydrogenation pathway is initiated already at the first methanol dehydrogenation step. On Pt(111) aqueous media, the most favorable dehydrogenation path occurs via the adsorbed hydroxymethyl CH_2OH intermediate, which is then further dehydrogenated to CO_{ads}. Alternatively, O−H bond cleavage leads to adsorbed methoxy, CH_3O_{ads}, which binds to Pt via the oxygen rather than the carbon atom. Methoxy can be dehydrogenated to H_2CO, leading to dissolved formaldehyde. On Pt(111), the stability of methoxy is much lower than that of hydroxymethyl, but, on a stepped Pt(211) surface, their stabilities are comparable, indicating that the presence of steps can significantly alter the reaction mechanism and the pathways chosen.

A similar idea, namely that the indirect and direct pathways involve different dehydrogenation precursors, that is, H_2COH_{ads} versus H_3CO_{ads}, respectively, was recently invoked by Iwasita et al. to explain the strong influence of adsorbed anions on the amount of formaldehyde formed during MeOH oxidation on Pt(111) at low overpotentials.[31,32] Adsorbed (bi)sulfate would effectively block "ensemble sites" for H_2COH_{ads} but not for CH_3O_{ads} formation, rationalizing the enhanced influence of the direct pathway in sulfuric acid versus perchloric acid. This explanation is based on the "ensemble site" theory, which has been quite popular in the methanol oxidation literature,[33,34] for instance, to explain the optimum Pt/Ru ratio (3:1) for PtRu catalysts[35,36] and to explain the particle-size dependence of supported nanoparticle catalysts. As the methanol oxidation rate was found to decrease with the nanoparticle size, Park et al. concluded that the decomposition of methanol requires an ensemble of terrace sites.[33] Tripković et al. found that, when the terrace width of Pt[n(111)×(100)] electrodes is decreased from $n = 6$ to $n = 3$ and 2 atoms per terrace (i.e., Pt(755), Pt(211), and Pt(331), respectively), the total methanol oxidation activity decreases,[34] in agreement with the conclusion of Park et al. However, recent results obtained in our group and results published by Shin and Korzeniewski seem to contradict these findings.[22,37] In both cases, increasing the step density resulted in an increase in the methanol oxidation rate.

In this paper, we study the formation of soluble intermediates at the basal planes of platinum and stepped Pt surfaces of [n(111)×(111)] orientation in both sulfuric and perchloric acid, using a tip-based modification of the DEMS technique[38−44] following the original design of Kita et al.[45] and the modifications introduced by Jambunathan et al.[46,47] The on-line electrochemical mass spectrometry (OLEMS) technique is described in more detail in ref 48. The main advantage of this technique over traditional DEMS is that experiments can be performed on bead-type single-crystal electrodes in the hanging meniscus configuration. Moreover, because the gas inlet is small and tip shaped, no differential pumping is necessary, thereby considerably reducing the detection limit of the system.[48] A disadvantage of the system is the longer delay between the measured current and the detected masses compared to the original DEMS setup. This delay is due to the electrolyte layer between the tip and the electrode and was also reported by Kita and Hiller.

With regard to detecting intermediates, however, the interference of species in solution poses a problem since mass fragments of methanol and formaldehyde coincide. This can be partially circumvented by measuring methylformate, which is formed by the reaction of methanol and formic acid and, thus, provides an indirect way of monitoring the activity of the direct oxidation pathway. However, results obtained by the groups of Korzeniewski[49,50] and Iwasita[31,32] indicate that formaldehyde is the most abundant soluble intermediate formed during the oxidation of methanol (next to CO_2). Measuring methylformate as an indicator for the direct oxidation pathway implies that formic acid is formed in the same pathway as formaldehyde, which is not obvious from the reaction mechanism. Yet, in aqueous solutions, formaldehyde is completely hydrolyzed to methylene glycol ($H_2C(OH)_2$),[51,52] which can dissociate to CO_{ads},[53] but which can also form formate on the Pt surface ($HCOO_{ads}$).[54−56] These adsorbed formate species can be oxidized to CO_2, but also imply the existence of formic acid in solution, thus indicating that the latter species would indeed be formed in the same reaction pathway as formaldehyde. Therefore, monitoring the formation of methylformate seems to be a viable procedure for measuring the activity of the direct methanol oxidation pathway.

By using the OLEMS setup for the methanol oxidation on stepped Pt electrodes of [n(111)×(111)] orientation and the basal planes in perchloric and sulfuric acid electrolytes, a more detailed insight into the structure sensitivity and the effect of specific anion adsorption on the direct oxidation pathway to soluble intermediates is gleaned. Additionally, the nature of the "ensemble sites" will be discussed. Our findings will be considered within the framework of the current views on platinum-catalyzed methanol electrooxidation, and we will propose a new overall oxidation scheme comprising the direct and indirect oxidation pathways.

2. Experimental Setup

For a detailed description of the OLEMS setup, we refer to ref 48. Briefly, the OLEMS setup consists of a small gas inlet tip made of PEEK in which a porous Teflon plug is pressed. The tip is connected to the mass spectrometer and can be brought in close proximity (10−20 μm) to the electrode in the hanging meniscus configuration by means of a micrometer positioning system and a camera.

The electrochemical cell used in the OLEMS experiments is a standard three-electrode cell made of glass, modified to allow the working electrode to be placed near the side of the cell in order to aid in the positioning of the OLEMS tip close to the electrode surface using the camera. The working electrodes were platinum bead-type single crystals, with the basal plane orientation and Pt[n(111)×(111)] (equivalent to Pt[m(111)×(110)] with $m = n - 1$) orientation (Pt(110), Pt(100), Pt(553) $n = 5$; Pt(554) with $n = 10$; and Pt(111) with $n = 200-500$), which were prepared according to Clavilier's method.[57] Prior to each measurement, the single-crystal electrode was flame annealed and cooled to room temperature in an argon (Hoekloos, N50)−hydrogen atmosphere, after which it was transferred to the electrochemical cell under the protection of a droplet of deoxygenated water.[58] The glassware, OLEMS tip, and glass

tubing were cleaned by boiling in a mixture of concentrated H_2SO_4/HNO_3, followed by repeated boiling with ultrapure water (Millipore MilliQ gradient A10 system, 18.2 MΩ cm, 2 ppb total organic carbon). The blank electrolytes, 0.5 M H_2SO_4 and 0.5 M $HClO_4$, were prepared with concentrated sulfuric and perchloric acid (Merck, "Suprapur") and ultrapure water. During measurements, the blank electrolyte was deoxygenated with argon (Hoekloos, N50). Measurements were performed at room temperature (22 °C) with a computer-controlled Autolab PGSTAT20 potentiostat (Ecochemie).

3. Results and Discussion

3.1. System Cleanliness and Surface Structure. As is customary, prior to each experiment, the structure of the surface and the cleanliness of the system were checked by measuring a blank cyclic voltammogram (BCV) of the electrodes under investigation. The resulting BCVs recorded in the sulfuric and perchloric acid electrolytes are shown in the Supporting Information (S1a−e) and agree well with those previously published in the literature.[13,16,28,30,59−65]

Equally important when using the OLEMS setup is the influence of the tip on the electrode surface and cleanliness of the system. This influence was checked by measuring and comparing BCVs of Pt(111) in the absence and presence (close proximity) of the tip. The resulting BCVs closely resemble each other, signifying that the tip does not contaminate the system significantly, and it has virtually no influence on the quality of the CVs recorded.[48] All of the obtained blank voltammograms satisfy the criteria of system cleanliness as proposed by Lebedeva et al.[26]

The performance of the OLEMS setup was checked by performing a CO-stripping experiment on Pt(111). The shape of the CO oxidation peak agrees well with the stripping curves reported in the literature.[26,48] Similar to the tip-based setups of Kita[66] and Hillier,[46] the corresponding signal for CO_2 (*m*/*z* 44, most intensive ion for CO_2) has a delay of ∼10−15 s between the CO oxidation peak and the peak in the recorded mass, which is characteristic for the present OLEMS setup.

3.2. Methanol Oxidation on Single-Crystal Platinum Surfaces. We wish to stress at the outset that our OLEMS setup does not yet allow for an accurate quantitative calibration. The intensity of the detected mass signals depends on many factors (e.g., the tip−electrode distance, the porosity of the Teflon plug, the quality of the vacuum inside the system, etc.[48]), which vary from one experiment to another. Consequently, a quantitative comparison of the recorded masses for the different surfaces is not possible at present. Therefore, the strategy we adopted was to compare the ratio between the masses of methylformate (*m*/*z* 60) and CO_2 (*m*/*z* 44) during the oxidation and, thereby, the relationship between the direct and indirect methanol oxidation pathway and the surface structure of the electrode. To avoid problems that arise from the delay time, we first compared the integrated charges obtained from the mass spectrometry cyclic voltammograms (MSCVs) for mass signals 60 and 44. Although informative with respect to the influence of the surface structure on the selectivity of the direct and indirect oxidation pathways, in this analysis, any potential-dependent information is lost.

The CVs and MSCVs recorded with the OLEMS on the basal Pt planes Pt(111), Pt(110), and Pt(100) in 0.5 M MeOH and 0.5 M H_2SO_4 at a scan rate of 2 $mV \cdot s^{-1}$ are shown in Figure 1, while the results for the stepped surfaces Pt(554) and Pt(553) together with Pt(111) are presented in Figure 2. The effect of specific anion adsorption on the electrooxidation reaction of methanol was investigated by repeating the experiments in 0.5 M $HClO_4$. The results for the basal planes in this electrolyte are presented in Figure 3 and the stepped surfaces in Figure 4. For the sake of clarity, we shall discuss the methanol oxidation on the basal planes and stepped platinum surfaces in separate sections. Figures 5 and 6 visualize a tentative relationship between the mass 60/44 ratio and the potential (obtained by dividing the measured *m*/*z* 60 signal by the *m*/*z* 44 signal) for the basal planes recorded in sulfuric and perchloric acid, respectively, while Figures 7 and 8 respectively represent similar curves for the stepped surfaces.

3.2.1. Methanol Oxidation on Basal Pt Planes. The CVs recorded on the basal planes of platinum (Figure 1a and 3a) correspond well with those recorded by Xia et al. in 0.1 M $HClO_4$ at a scan rate of 50 $mV \cdot s^{-1}$,[67] and display an increase in (maximum) activity toward methanol oxidation in the order Pt(111) < Pt(110) < Pt(100). However, our results are in contrast to results published by Herrero et al., who reported an increasing activity in the order Pt(111) < Pt(100) < Pt(110) in sulfuric as well as perchloric acid.[13] Comparing the Pt(110) BCV of Herrero et al. to ours reveals significant differences in the surface structure and system cleanliness. We believe this suggests that the Pt(110) surface used by Herrero et al. was more disordered than ours and consisted mostly of the (1 × 2) reconstructed surface and other defects. Marković et al. indeed reported an increased activity for the oxidation of CO on the reconstructed (1 × 2) Pt(110) surface compared to (1 × 1) Pt(110).[68] Moreover, the maximum current density of the hydrogen adsorption/desorption peaks suggests that the cleanliness of the system was not optimal. On the basis of the onset of the reaction (<0.6 V vs RHE), the Pt(110) surface seems to be the most active, followed by the Pt(111) and Pt(100) surfaces.

Turning to product formation, Figure 1b shows that, on Pt(111), small amounts of methylformate can be detected. In an in situ Fourier transform infrared (FTIR) study, Xia et al. also identified weak bands corresponding to methylformate on Pt(111) during the electrooxidation of methanol (0.1 M) in 0.1 M $HClO_4$.[67] As the current density increases from Pt(110) to Pt(100) (Figure 1c,d), the amounts of CO_2 and methylformate produced increase. It is noteworthy that, on Pt(111), CO_2 can be detected in the negative going scan at potentials as low as 0.4 V versus RHE, which is well below the potential at which surface-adsorbed CO is oxidized. Since the delay of the system for the detection of CO_2 is on the order of seconds, we do not believe that the CO_2 signal detected at 0.4 V is entirely due to the delay and tailing of the *m*/*z* 44 signal. Moreover, close examination of the *m*/*z* 44 signal obtained on Pt(111) in sulfuric acid always reveals a slight increase in signal between 0.43 and 0.35 V versus RHE in the negative going scan, which cannot be explained by delay or tailing. This observation contradicts earlier findings reported by the group of Vielstich[18] and indicates that a parallel pathway is active at low potentials. Jarvi et al. also reported nonzero CO_2 yields for potentials where surface-adsorbed CO is stable on Pt(100) and Pt(111).[4,69] In addition, our findings agree well with the results published by the groups of Wieckowski[13,14,30] and Stuve,[16,17,69] who, on the basis of a coulometric analysis, independently concluded that a second pathway to CO_2, not involving surface-bonded CO, must be active at low potentials.

As is well-known, changing the electrolyte from sulfuric to perchloric acid leads to an increase in the overall current densities recorded due to the lower adsorption strength of the latter anion (see Figure 3a). The intensities of the *m*/*z* 60 and 40 signals shown in Figure 3b−d are correspondingly higher.

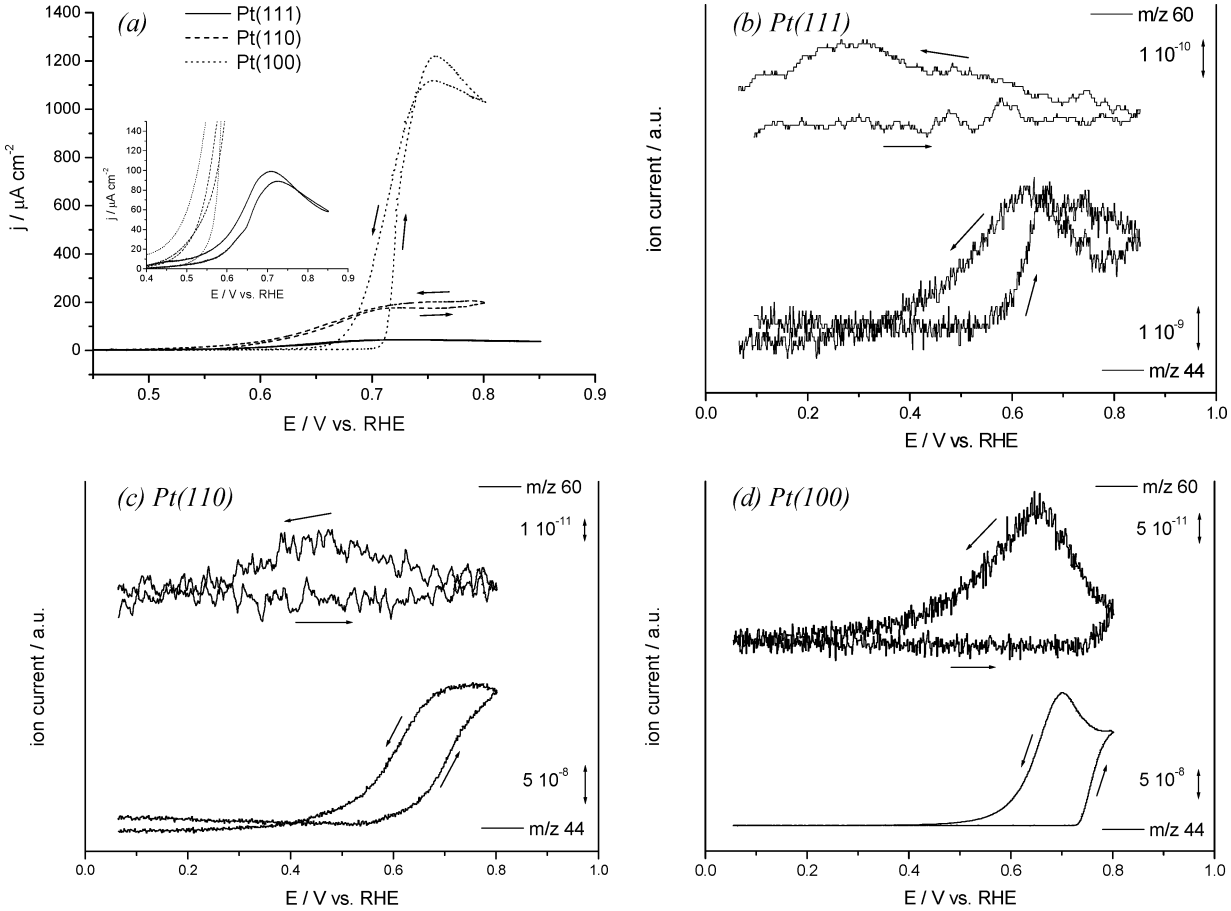

Figure 1. (a) CVs of Pt(111) (solid line), Pt(110) (dashed line), and Pt(100) (dotted line) in 0.5 M MeOH and 0.5 M H_2SO_4 at a scan rate of 2 $mV \cdot s^{-1}$. The top mass shown in the associated MSCVs for Pt(111) (b), Pt(110) (c), and Pt(100) (d) displays the methylformate signal (*m*/*z* 60), and the bottom one displays the carbon dioxide signal (*m*/*z* 44). The inset shows a zoom of the Pt(111) CV.

As was mentioned earlier, by calculating the ratio between the amount of methylformate and CO_2 detected during the voltammetric scan, the effect of surface structure and specific anion adsorption on the methanol oxidation pathway can be investigated without the interference of the typical OLEMS delay. The mass 60/44 ratios were calculated by dividing the total amount of methylformate corresponding to the *m*/*z* 60 MSCV (obtained by integration of the MSCV from the baseline) with the *m*/*z* 44 signal (obtained in the same way). The calculated values, which are an average of 2−3 independent measurements, are given in Table 1.

As in the positive going scan, no soluble products or CO_2 are formed at low potentials; the signal detected between 0 and 0.5 V versus RHE depends only on the background pressure in the OLEMS system. If the background pressure is constant, the detected constant mass signals can be used as baselines for the integration procedure. For background pressure fluctuations, the baseline is corrected accordingly. The tabulated values obtained accordingly have an average deviation of less than 10−20%, lending credit to the reliability of the method.

In sulfuric acid, the values for the mass 60/44 ratio clearly demonstrate that, although Pt(100) has the highest overall activity, it has the lowest selectivity toward the direct oxidation pathway (through soluble intermediates). Compared to the CO_2 formation, both Pt(111) and Pt(110) produce reasonably large quantities of methylformate, suggesting that the direct pathway plays an important role in the oxidation of methanol on these surfaces. The results for Pt(111) and Pt(110) agree well with the literature, as both formaldehyde and formic acid have been reported to be among the primary species formed.[7,31,32] Using a combination of chronoamperometry, fast cyclic voltammetry, and theoretical methods, Cao et al.[30] also found a low selectivity toward the direct methanol oxidation pathway on Pt(100), while both Pt(111) and Pt(110) display a relatively high selectivity for the direct pathway. Interestingly, Herrero et al. observed that Pt(100) reacts differently compared to Pt(111) and Pt(110).[13] On the latter two surfaces, they reported a Tafel slope of 120 $mV \cdot dec^{-1}$, while 60 $mV \cdot dec^{-1}$ was found for Pt(100), suggesting a different rate-determining step on the (100) surface.

Although the CVs recorded in perchloric acid appear to be similar to those recorded in sulfuric acid media, a markedly different trend in the methylformate−carbon dioxide ratio is observed. Compared to sulfuric acid, the Pt(110) and Pt(100) surfaces are more active toward the direct oxidation pathway, as is apparent from the increased mass 60/44 ratio in Table 1, while Pt(111) favors the indirect oxidation pathway.

Batista et al. explained the enhanced role of the direct pathway on Pt(111) in sulfuric acid by a lack of multiple coordination sites for methanol adsorption due to strong adsorption of (bi)-sulfate, leading to the formation of soluble intermediates rather than CO.[31,32] It was suggested that the dissociative adsorption of methanol on an ensemble of empty surface sites favors C−H bond scission and, thus, leads to CO formation. If such an "ensemble site" is absent, or if only a single adsorption site is available, methanol would interact with the surface by O−H bond scission and lead to the formation of soluble intermediates. This theory implies a considerable dissociation of methanol on (111) terrace sites, which seems to conflict with the idea that the decomposition of methanol preferably takes place at steps (see ref 22). Perhaps the reaction rate on the terraces is much

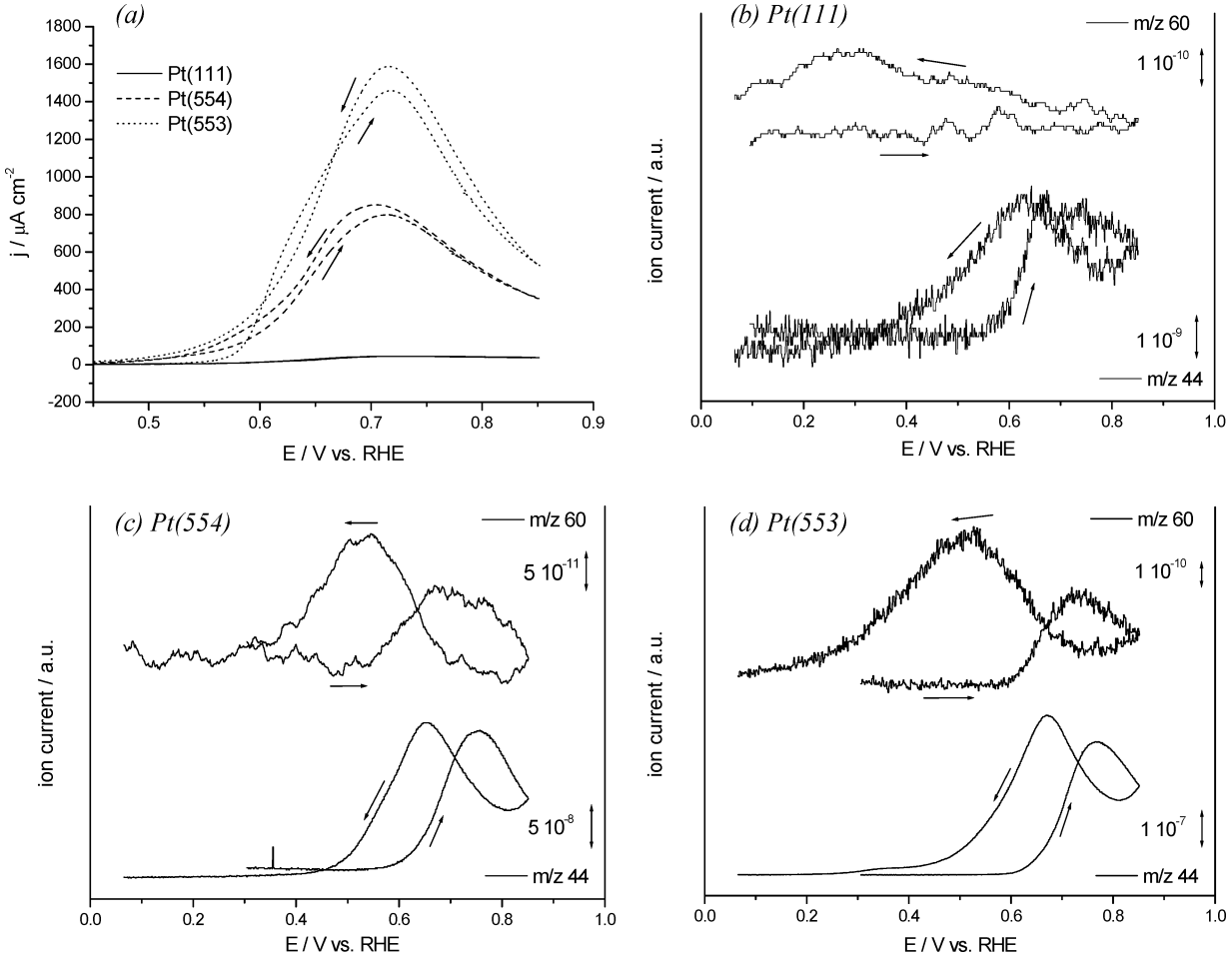

Figure 2. (a) CVs of Pt(111) (solid line), Pt(554) (dashed line), and Pt(553) (dotted line) in 0.5 M MeOH and 0.5 M H_2SO_4 at a scan rate of 2 $mV \cdot s^{-1}$. The top mass shown in the associated MSCVs for Pt(111) (b), Pt(110) (c), and Pt(100) (d) displays the methylformate signal (*m*/*z* 60), and the bottom one displays the carbon dioxide signal (*m*/*z* 44).

slower than that on the steps, but still plays a prominent role in the formation of intermediates on surfaces with a low step or defect density.

Following the anion theory proposed by Batista et al., reducing the anion adsorption strength by switching from sulfuric acid electrolyte to perchloric acid should lead to an increase in the number of ensemble sites available for methanol decomposition to CO and, accordingly, to a lower mass 60/44 ratio. Indeed, as is apparent from Table 1, the mass 60/44 ratio for Pt(111) in sulfuric acid is twice as high as that in perchloric acid. On all other surfaces, however, the formation of soluble intermediates is favored in perchloric acid media.

These findings indicate that, if no adsorbed CO is present on the surface, competitive adsorption between (bi)sulfate and methanol will occur. Since (bi)sulfate adsorbs strongly on the (111) surface and only a few crystalline defects are present, the total reaction rate is low and the number of sites where methanol decomposes to soluble intermediates via O−H bond scission will be relatively high compared to the number of ensemble sites on which methanol can decompose to CO via C−H bond scission. Additionally, Olivi et al. suggested that oxidation of formaldehyde on Pt(110) and Pt(100) may occur by two different processes:[70] one involving the formation of CO_{ads} and the other involving direct oxidation of methylene glycol. Since methylene glycol oxidation to CO_2 can occur at lower potentials on Pt(100) but is inhibited on Pt(110), the former surface produces more CO_2 and, accordingly, has a mass 60/44 ratio lower than that of the latter.

The mass 60/44 ratios presented in Table 1 illustrate the effect of the structure sensitivity on the methanol oxidation pathway integrated over the forward and back potential scans. To give insight into the potential dependence of the direct and indirect pathway on each surface, Figures 5 and 6 show the potential-dependent mass 60/44 ratios of the basal planes of platinum recorded in sulfuric and perchloric acid, respectively. In these figures, the ratio of the background levels detected by the mass spectrometer was set to zero. Therefore, the figures depict the deviation of the *m*/*z* 60/44 ratio (Δ ratio) from the zero line, rather than the actual ratios. We would like to note at this point that, even though the delay time of the OLEMS is considerable compared to traditional DEMS techniques (10−15 s), we believe that it does not significantly influence trends observed in our results. Nevertheless, the delay time should be taken into account, and the displayed results should be taken as general trends.

In the positive going scan, poisoning CO is oxidized to CO_2, which results in a decrease in the mass 60/44 ratio on all surfaces. In the return scan, competitive adsorption between (bi)-sulfate and methanol reduces the number of free ensemble sites and, thus, favors the formation of soluble intermediates, as can be seen by the increase in the *m*/*z* 60/44 ratio between 0.85 and 0.6 V versus RHE. Figure 5 demonstrates that, in sulfuric acid, Pt(111) has the highest methylformate/CO_2 ratio at high potentials (>0.6 V vs RHE) and, thus, favors the direct methanol oxidation pathway. At lower potentials, CO is stable on the

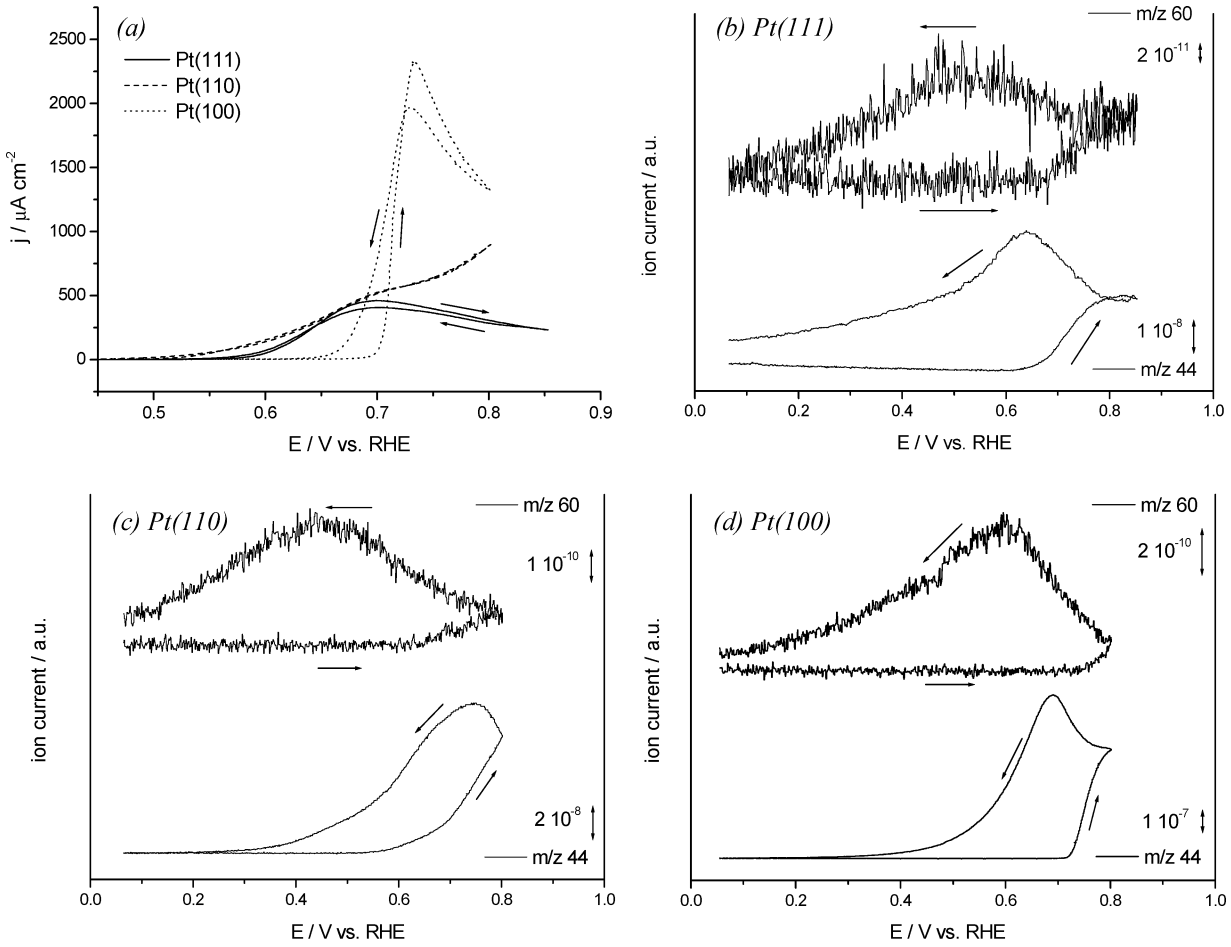

Figure 3. (a) CVs of Pt(111) (solid line), Pt(110) (dashed line), and Pt(100) (dotted line) in 0.5 M MeOH and 0.5 M $HClO_4$ at a scan rate of 2 mV·s^{-1}. The top mass shown in the associated MSCVs for Pt(111) (b), Pt(110) (c), and Pt(100) (d) displays the methylformate signal (*m*/*z* 60), and the bottom one displays the carbon dioxide signal (*m*/*z* 44).

surface, and only methylformate (or CO_2 formed in the direct oxidation pathway) can be detected.

Interestingly, the maxima in the *m*/*z* 60/44 ratio for Pt(110) and Pt(100) lie at ~0.45−0.5 V, while Pt(111) shows a maximum at ~0.25−0.3 V versus RHE in the negative going scan. Below 0.45 V, (bi)sulfate starts to desorb from the (111) surface, which may result in an increase in the number of available sites for methanol decomposition. Methanol adsorbing on these sites can be converted to either CO_{ads} or soluble intermediates, which results in an increase in the methylformate/CO_2 ratio.

In the high-potential region, the *m*/*z* 60/44 ratio decreases when going from Pt(111) to Pt(110) and Pt(100) as a result of the increasing activity toward the indirect pathway in that order. In the negative going scan, even though the (100) surface shows the highest amount of *m*/*z* 60, the relative importance of the direct pathway activity on this surface is lower than that of Pt(110) (as is apparent from Table 1).

In perchloric acid, the oxidation characteristics of the surfaces change markedly (see Figure 6). In this medium, the order of the relative selectivity toward the direct oxidation pathway is Pt(111) < Pt(100) < Pt(110). The decrease in the mass ratio for Pt(111) in the negative going scan can be ascribed to a slower decrease in the CO_2 signal compared to the *m*/*z* 60 signal, as is visible in the corresponding MSCV (Figure 3b), which may be due to CO_2 formation by oxidation of soluble intermediates at low potentials. Despite the fact that the calculated values for Pt(111) and Pt(100) presented in Table 1 are quite similar, Figure 6 demonstrates that Pt(100) produces relatively more soluble intermediates at lower potentials than Pt(111).

3.2.2. Methanol Oxidation on Stepped Pt[n(111)×(111)]-Type Electrodes. The CVs of the stepped electrodes in sulfuric acid (Figure 2a) display all the characteristics of the CVs recorded previously in 25 mM MeOH at 50 mV·s^{-1} and show the expected increase in the maximum current density for increasing step density.[22] Since the scan rate used here is 2 mV·s^{-1}, the hydrogen region is almost completely blocked by CO or other MeOH decomposition products.[22] As was anticipated, the total methanol oxidation activity in perchloric acid is higher than that in sulfuric acid (compare Figure 2a to Figure 4a).

The MSCVs presented in Figures 2b−d and 4b−d indicate that, apart from the expected increase in the CO_2 signal, the methylformate signal also increases with the step density (see also Table 1). It was mentioned in the previous section that, on well-defined Pt(111) in sulfuric acid, only a small quantity of methylformate can be detected, even at the relatively high methanol concentrations used in this study, but the ratio between methylformate and CO_2 is relatively high compared to the stepped surfaces. In the presence of (bi)sulfate, a comparison of the methylformate/CO_2 ratios for Pt(554) and Pt(111) shows that introducing steps in the (111) plane results in an increase in the prominence of the indirect pathway. This observation may be rationalized by the disruption of the (ordered) anion layer due to the presence of the step sites. As the step density is increased further from Pt(554) to Pt(553) in both electrolytes, the mass 60/44 ratios increase, which strongly suggests that steps

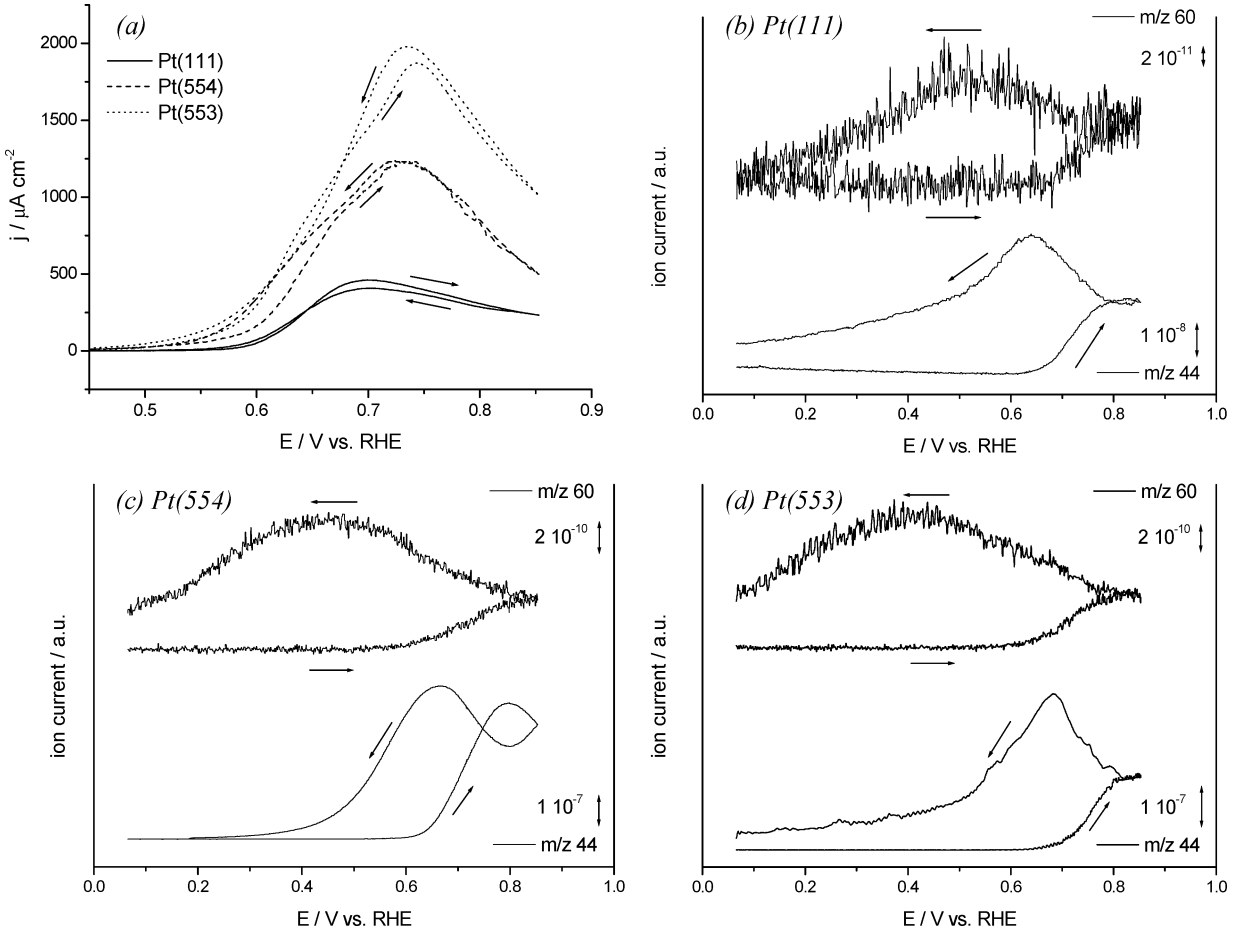

Figure 4. (a) CVs of Pt(111) (solid line), Pt(554) (dashed line), and Pt(553) (dotted line) in 0.5 M MeOH and 0.5 M $HClO_4$ at a scan rate of 2 $mV \cdot s^{-1}$. The top mass shown in the associated MSCVs for Pt(111) (b), Pt(554) (c), and Pt(553) (d) displays the methylformate signal (*m*/*z* 60), and the bottom one displays the carbon dioxide signal (*m*/*z* 44).

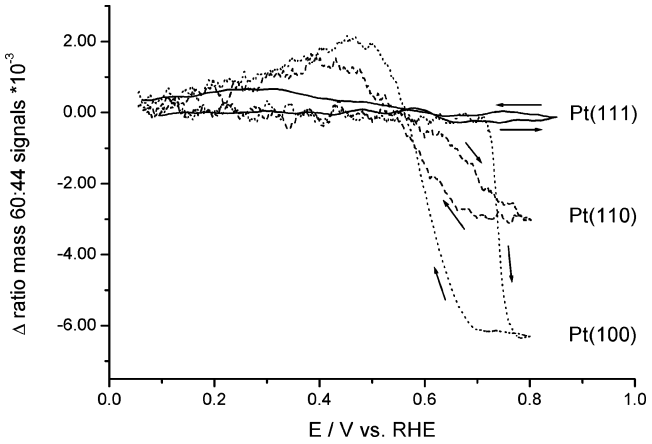

Figure 5. Potential-dependent plot of the *m*/*z* 60/44 ratio measured for Pt(111) (solid line), Pt(110) (dashed line), and Pt(100) (dotted line) recorded in 0.5 M MeOH and 0.5 M H_2SO_4 at a scan rate of 2 $mV \cdot s^{-1}$.

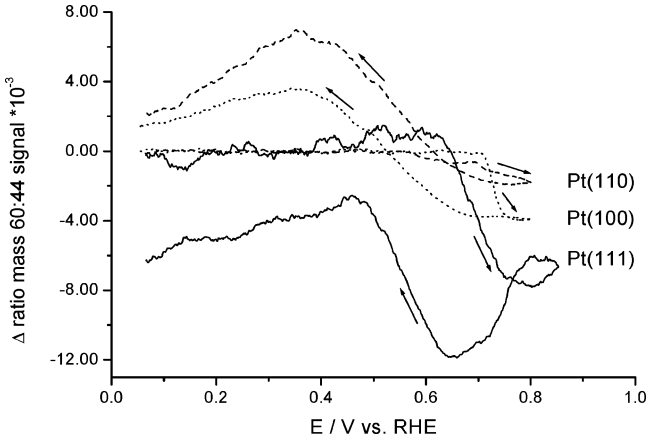

Figure 6. Potential-dependent plot of the *m*/*z* 60/44 ratio measured for Pt(111) (solid line), Pt(110) (dashed line), and Pt(100) (dotted line) recorded in 0.5 M MeOH and 0.5 M $HClO_4$ at a scan rate of 2 $mV \cdot s^{-1}$.

themselves catalyze the formation of intermediates during the methanol oxidation. On the basis of experiments with polycrystalline, dispersed nanoparticle, and blackened Pt electrodes, numerous authors have already suggested that steps and crystalline defects catalyze the direct pathway.[19−21] DFT calculations using a (211) surface indicated that the prevalence of the direct oxidation pathway towards positive potentials may be due to preferred initial O−H cleavage over defect sites.[30] Note, however, that the steps on Pt(211) are of (100) orientation, which is precisely the surface which shows the lowest preference toward the direct oxidation pathway.

In perchloric acid, the amount of CO_2 recorded on Pt(111) is higher relative to the amount of methylformate compared to that in sulfuric acid media, in agreement with the observations of Batista et al.[31,32] As the step density is increased, the calculated methylformate/CO_2 ratio steadily increases, illustrating that, in the absence of specifically adsorbing anions, steps catalyze the direct oxidation pathway of methanol to intermediates such as formic acid and formaldehyde.

The potential-dependent *m*/*z* 60:44 ratios for the stepped surfaces in sulfuric and perchloric acid are shown in Figures 7 and 8, respectively. In the positive going scan at potentials higher

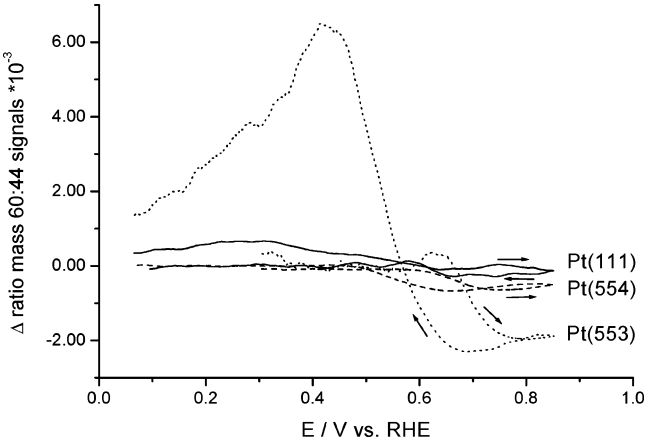

Figure 7. Potential-dependent plot of the *m*/*z* 60/44 ratio measured for Pt(111) (solid line), Pt(554) (dashed line), and Pt(553) (dotted line) recorded in 0.5 M MeOH and 0.5 M H_2SO_4 at a scan rate of 2 mV·s^{-1}.

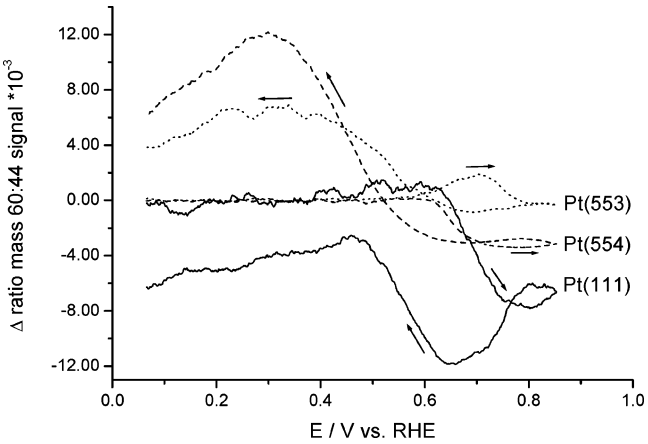

Figure 8. Potential-dependent plot of the *m*/*z* 60/44 ratio measured for Pt(111) (solid line), Pt(554) (dashed line), and Pt(553) (dotted line) recorded in 0.5 M MeOH and 0.5 M $HClO_4$ at a scan rate of 2 mV·s^{-1}.

TABLE 1: Ratio of the Methylformate (*m*/*z* 60) and Carbon Dioxide (*m*/*z* 44) Mass Signals Calculated for Pt(111), Pt(110), Pt(100), Pt(554), and Pt(553) in 0.5 M H_2SO_4 and 0.5 M $HClO_4$ Integrated over One Voltammetric Cycle at 2 mV·s^{-1}[a]

	mass 60/44 ratio * 10^{-3}	
surface	H_2SO_4	$HClO_4$
Pt(111)	3.3	1.5
Pt(110)	2.4	6.8
Pt(100)	1.2	1.7
Pt(554)	1.4	1.9
Pt(553)	1.8	3.1

[a] The values given are an average of 2−3 separate experiments.

than 0.6 V versus RHE in the presence of (bi)sulfate, Pt(111) has the highest and Pt(553) has the lowest *m*/*z* 60:44 ratio, indicating that the influence of the indirect oxidation pathway increases with the step density. In the return scan, the results indicate that the selectivity toward the direct oxidation pathway increases in the order Pt(554) < Pt(111) < Pt(553). In perchloric acid, the lower adsorption strength of perchlorate results in a change in this order to Pt(111) < Pt(554) < Pt(553). In general, compared to sulfuric acid media, in the perchloric acid electrolyte, the relative importance of the indirect pathway in the positive going scan and the direct oxidation pathway in the negative going scan are enhanced.

These findings illustrate the varying effect of anion adsorption on the oxidation characteristics at steps and terraces. On (111) terraces, anion adsorption suppresses the formation of CO in the indirect pathway. On step sites, however, the strongly adsorbing (bi)sulfate anion seems to inhibit the direct pathway compared to perchlorate. It is possible that (bi)sulfate indirectly blocks the steps, or hinders the approach of methanol to the steps, which by themselves catalyze the direct oxidation pathway, resulting in less methylformate being formed. In perchloric acid, methanol is allowed easy access to the reactive step, which leads to more soluble intermediates being formed. Finally, reducing the terrace width results in a decrease in the role of the indirect oxidation pathway.

Further hints on the role of steps and defects in the formation of intermediates during the electrooxidation of methanol can be obtained from the position of the maxima of the mass signals. In the positive going scan, the potential of the *m*/*z* 60 maximum in sulfuric acid media lies considerably lower than that of the *m*/*z* 44 signal maximum, signifying that intermediates can already be formed at potentials well below the oxidation potential of adsorbed CO.[26] Moreover, in the negative going scan, the methylformate maximum recorded on Pt(554) in 0.5 M H_2SO_4 lies at ∼0.54 V and at ∼0.52 V versus RHE on Pt(553), and that in $HClO_4$ lies at ∼0.48 and 0.40 V, respectively, indicating that, on surfaces with a higher step density, the direct pathway is active at lower potentials. The delay in the *m*/*z* 60 signal may also be attributed to an accumulation of methylformate in the electrolyte near the tip. However, the differences in the potential of the *m*/*z* 60 maximum and the maximum current density are approximately 115 mV for Pt(554) and 150 mV for Pt(553) in 0.5 M H_2SO_4, which, at a scan rate of 2 mV·s^{-1}, implies delay times of 57 and 75 s, respectively. In perchlorate containing electrolytes, these delay times are even higher. Because these delay times are considerably longer than previously reported typical delay times of the OLEMS system (see ref 48), we believe that they are not due to slow diffusion of methylformate from the electrode to the mass spectrometer, but rather hint at the formation of methylformate at potentials considerably lower than the maximum in the current density in the negative going scan.

Finally, it is noteworthy that the oxidation current densities on Pt(554) and Pt(553) are higher than those on Pt(110). Apparently, stepped surfaces of [*n*(111)×(111)] orientation are more active than the [110] steps themselves. This may indicate that, to decompose methanol to CO, the combination of a step site and a neighboring terrace site is required. If only step or terrace adsorption sites are available, methanol preferably decomposes to soluble intermediates.

3.3. Methanol Oxidation Scheme. In this section, we would like to draw up a detailed scheme for methanol oxidation based on the results presented here as well as previously published results. Scheme 1 incorporates the formation of soluble intermediates such as formaldehyde and formic acid, but also assists in understanding the structure sensitivity of the reaction and the effects of anion adsorption. Scheme 1 is essentially an extension of the scheme suggested recently by Cao et al.,[30] incorporating as an additional feature the presumed pathways for the formation of formaldehyde and formic acid.

As in the scheme of Cao et al.,[30] it is suggested that the decision between the direct and indirect pathways is made at the initial dehydrogenation step, that is, the breaking of the O−H or C−H bond, respectively. The dehydrogenation step of methanol to hydroxymethyl, reaction 1, was found to be the rate-determining step on Pt(111) and Pt(110),[13,71] while, on Pt(100), reaction 2 was assumed to be rate determining.[13] Our results indicate that (111) terraces in the absence of strongly

SCHEME 1

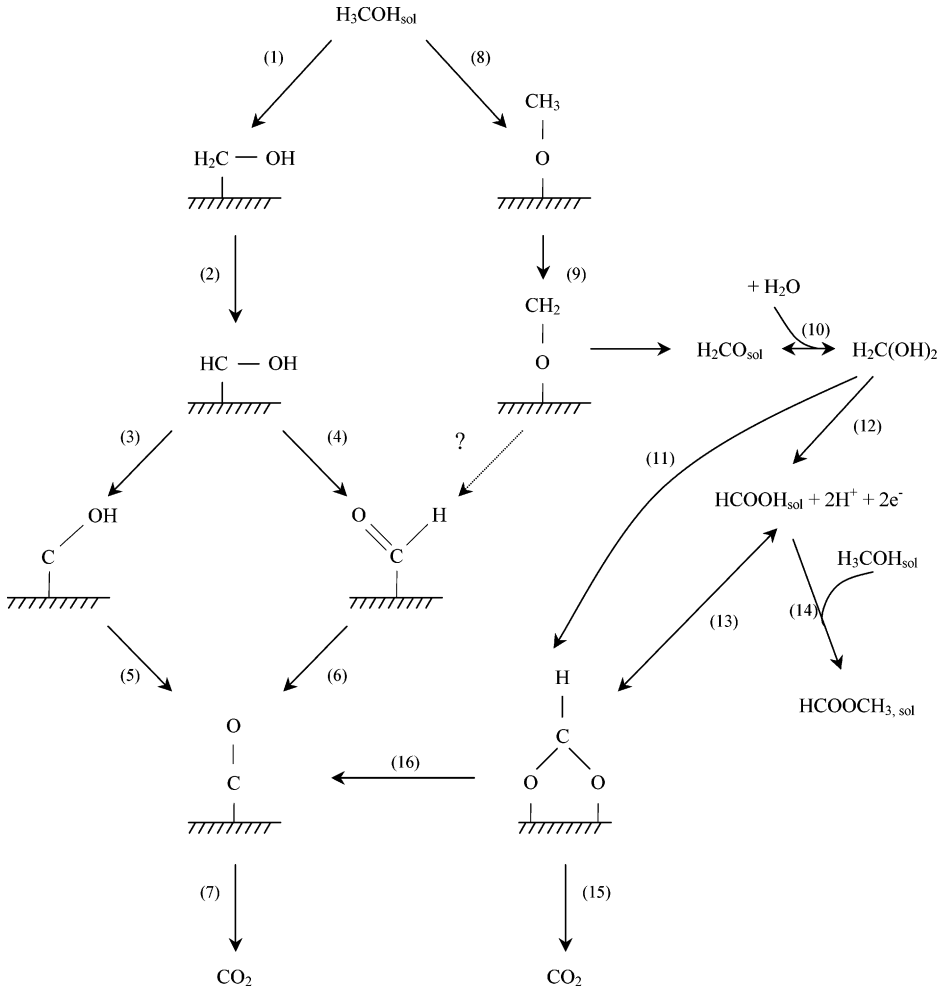

adsorbing anions (i.e., (bi)sulfate), as well as Pt(100), favor reaction 1. The presence of an H/C/O species has been extensively discussed in the literature.[1,8,10,72−76] Whether this H/C/O species is the HCO formed in reaction 3 or the COH formed in reaction 4 is, at present, still unclear. However, it is generally accepted that, ultimately, CO_{ads} is formed at low potentials, which acts as a surface poison.[1,4−7] Depending on the coverage and potential, linearly, bridge-, or multifold-bonded CO can be formed, with the most prevalent configuration being linearly bonded CO.[55,77]

Under UHV conditions, the dehydrogenation reaction 8 to methoxy is known to occur readily.[78−82] Under electrochemical conditions, our results indicate that O−H bond scission occurs preferably on Pt(111) in sulfuric acid media and on steps of (110) orientation in the absence of (bi)sulfate. On Pt(110), reaction 8 also seems relatively important, regardless of the electrolyte. Calculations by Cao et al. indicate that (100)-type steps also catalyze the O−H bond scission, even though the Pt(100) surface itself seems to favor C−H bond scission.[30] Further dehydrogenation of H_3CO_{ads} leads to H_2CO_{ads} (reaction 9), which may desorb as formaldehyde. Whether or not H_2CO_{ads} reacts to a H/C/O species is not clear. Once formed, formaldehyde is completely hydrated rapidly to methylene glycol (reaction 10).[51,52] Since adsorbed CO was found during the oxidation of formaldehyde on platinum, Miki et al. suggested that methylene glycol dissociates to CO_{ads},[54] although Olivi et al. proposed a reaction involving nonhydrated formaldehyde.[83] Olivi et al. also reported that the Pt(100) surface is more active for the $H_2C(OH)_2$ oxidation than the Pt(110) surface.[70] This would agree well with our OLEMS data. If Pt(100) is more active for the oxidation of methylene glycol (formed during the oxidation of methanol) to CO_2 than Pt(110), less formic acid would be produced on this surface, and, hence, a lower ratio of methylformate/CO_2 should be recorded, as indeed is the case.

Finally, our scheme explains why Osawa and co-workers observed the formation of formate on platinum surfaces during the electrooxidation of methanol, formic acid, and formaldehyde (methanol: reactions 8−12; formic acid: reaction 13; and formaldehyde: reactions 10+11 and 10+12+13).[54−56] Furthermore, they proposed that formate may react to either CO_2 or CO_{ads} (reactions 5 and 16, respectively). The formation of formic acid may occur via desorption of formate from the surface or by direct electrooxidation of $H_2C(OH)_2$, and ultimately leads to the production of methylformate by a reaction with methanol (reaction 14).

We believe that Scheme 1 presents a fairly complete and consistent picture of the methanol oxidation mechanism on platinum. The reaction path following reactions 1 to 7 would constitute what is commonly referred to as the indirect methanol oxidation pathway, while the series of reactions from 8 to 15 represent the direct methanol oxidation pathway.

4. Conclusions

In this paper, we have investigated the selectivity and structure sensitivity of the methanol oxidation pathways on basal planes and stepped platinum single-crystal electrodes by monitoring the mass fractions of CO_2 (*m*/*z* 44) and methylformate (*m*/*z* 60,

formed from CH_3OH + HCOOH) in 0.5 M H_2SO_4 and 0.5 M $HClO_4$ using OLEMS. We can summarize our main conclusions as follows:

- Contrary to previously published literature, in sulfuric and perchloric acid, the (maximum) reactivity for the methanol oxidation reaction increases in the order Pt(111) < Pt(110) < Pt(100).
- In sulfuric acid media, the oxidation of methanol on Pt(111) seems to show a preference for the direct oxidation pathway, while, in perchloric acid media, the indirect pathway through CO_{ads} appears to be favored. These observations may be explained by assuming that strongly adsorbing anions reduce the amount of available "ensemble sites" necessary for the dissociative adsorption of methanol via C−H bond cleavage, which normally would lead to CO_{ads} formation. If only single adsorption sites (or insufficient ensemble sites) are available for the adsorption of methanol, O−H bond scission is favored, leading to the formation of soluble intermediates. Therefore, in the presence of weakly adsorbing anions, the indirect oxidation pathway is favored, as is the case for perchlorate.
- In the absence of specifically adsorbed anions, steps of (110) orientation are suggested to catalyze the formation of soluble intermediates. In sulfuric acid, introducing steps in the (111) terraces leads to an increase in the relative rate of the indirect oxidation pathway, presumably as a result of disruption of the anion adlayer. However, with the exception of Pt(111), the relative importance of the direct oxidation pathway is always higher in perchloric acid compared to sulfuric acid.
- Since the activity of well-ordered Pt(110) is lower than that of the stepped surfaces Pt(554) and Pt(553) in both electrolytes, methanol appears to decompose preferably at step sites that are directly neighbored by a (111) terrace site. This combination, that is, a step plus terrace site, seems to be a particularly favorable "ensemble site" for methanol decomposition.

Finally, on the basis of the literature and the OLEMS data, a detailed scheme of the methanol oxidation mechanism was presented. The scheme incorporates a parallel pathway, the formation of soluble intermediates such as formic acid and formaldehyde, the selectivity and structure sensitivity of the formation of these intermediates, the effect of anion adsorption, as well as the occurrence of surface-adsorbed intermediates as detected by IR spectroscopy. Further improvement of the delay time by reducing the system volume and streamlining the tip−mass-spectrometry connection would improve the accuracy of the measurements and will, therefore, be a focus point for future research. Furthermore, a chronoamperometric analysis would provide more detailed information on the kinetics of the direct oxidation pathway.

Acknowledgment. This research was supported by the Netherlands Foundation for Scientific Research (NWO).

Supporting Information Available: BCVs of Pt(111) (a), Pt(110) (b), Pt(100) (c), Pt(554) (d), and Pt(553) (e) in 0.5 M H_2SO_4 (solid line) and 0.5 M $HClO_4$ (dashed line) at a scan rate of 50 $mV \cdot s^{-1}$. This material is available free of charge via the Internet at http://pubs.acs.org.

References and Notes

(1) Parsons, R.; VanderNoot, T. *J. Electroanal. Chem.* **1988**, *257*, 9.
(2) Hamnett, A. *Catal. Today* **1997**, *38*, 445.
(3) Lipkowski, J.; Ross, P. N. *Electrocatalysis: Frontiers in Electrochemistry*; Wiley: New York, 1998.
(4) Jarvi, T. D.; Sriramulu, S.; Stuve, E. M. *J. Phys. Chem. B* **1997**, *101*, 3649.
(5) Hamnett, A.; *Compr. Chem. Kinet.* **1999**, 635.
(6) Markovic, N. M.; Ross, P. N. *Surf. Sci. Rep.* **2002**, *45*, 117.
(7) Iwasita, T. *Electrochim. Acta* **2002**, *47*, 3663.
(8) Willsau, J.; Wolter, O.; Heitbaum, J. *J. Electroanal. Chem. Interfacial Electrochem.* **1985**, *185*, 163.
(9) Iwasita, T.; Vielstich, W.; Santos, E. *J. Electroanal. Chem. Interfacial Electrochem.* **1987**, *229*, 367.
(10) Wilhelm, S.; Iwasita, T.; Vielstich, W. *J. Electroanal. Chem. Interfacial Electrochem.* **1987**, *238*, 383.
(11) Lopes, M. I.; Fonseca, I.; Olivi, P.; Beden, B.; Hahn, F.; Leger, J. M.; Lamy, C. *J. Electroanal. Chem.* **1993**, *346*, 415.
(12) Gerischer, H., Tobias, C. W., Eds. *Advances in Electrochemical Science and Engineering*; Wiley−VCH: New York, 1990; Vol. 1.
(13) Herrero, E.; Franaszczuk, K.; Wieckowski, A. *J. Phys. Chem.* **1994**, *98*, 5074.
(14) Herrero, E.; Chrzanowski, W.; Wieckowski, A. *J. Phys. Chem.* **1995**, *99*, 10423.
(15) Lu, G. Q.; Chrzanowski, W.; Wieckowski, A. *J. Phys. Chem. B* **2000**, *104*, 5566.
(16) Sriramulu, S.; Jarvi, T. D.; Stuve, E. M. *Electrochim. Acta* **1998**, *44*, 1127.
(17) Sriramulu, S.; Jarvi, T. D.; Stuve, E. M. *J. Electroanal. Chem.* **1999**, *467*, 132.
(18) Vielstich, W.; Xia, X. H. *J. Phys. Chem.* **1995**, *99*, 10421.
(19) Wang, H.; Loffler, T.; Baltruschat, H. *J. Appl. Electrochem.* **2001**, *31*, 759.
(20) Wang, H.; Baltruschat, H. *Proc. − Electrochem. Soc.* **2001**, *2001-4*, 50.
(21) Wang, H.; Wingender, C.; Baltruschat, H.; Lopez, M.; Reetz, M. T. *J. Electroanal. Chem.* **2001**, *509*, 163.
(22) Housmans, T. H. M.; Koper, M. T. M. *J. Phys. Chem. B* **2003**, *107*, 8557.
(23) Gilman, S. *J. Phys. Chem.* **1964**, *68*, 70.
(24) Massong, H.; Tillmann, S.; Langkau, T.; Abd El Meguid, E. A.; Baltruschat, H. *Electrochim. Acta* **1998**, *44*, 1379.
(25) Akemann, W.; Friedrich, K. A.; Linke, U.; Stimming, U. *Surf. Sci.* **1998**, *402−404*, 571.
(26) Lebedeva, N. P.; Koper, M. T. M.; Herrero, E.; Feliu, J. M.; van Santen, R. A. *J. Electroanal. Chem.* **2000**, *487*, 37.
(27) Lebedeva, N. P.; Koper, M. T. M.; Feliu, J. M.; van Santen, R. A. *J. Electroanal. Chem.* **2002**, *524−525*, 242.
(28) Lebedeva, N. P.; Koper, M. T. M.; Feliu, J. M.; van Santen, R. A. *J. Phys. Chem. B* **2002**, *106*, 12938.
(29) Lebedeva, N. P.; Rodes, A.; Feliu, J. M.; Koper, M. T. M.; van Santen, R. A. *J. Phys. Chem. B* **2002**, *106*, 9863.
(30) Cao, D.; Lu, G. Q.; Wieckowski, A.; Wasileski, S. A.; Neurock, M. *J. Phys. Chem. B* **2005**, *109*, 11622.
(31) Batista, E. A.; Malpass, G. R. P.; Motheo, A. J.; Iwasita, T. *Electrochem. Commun.* **2003**, *5*, 843.
(32) Batista, E. A.; Malpass, G. R. P.; Motheo, A. J.; Iwasita, T. *J. Electroanal. Chem.* **2004**, *571*, 273.
(33) Park, S.; Xie, Y.; Weaver, M. J. *Langmuir* **2002**, *18*, 5792.
(34) Tripkovic, A. V.; Popovic, K. D. *Electrochim. Acta* **1996**, *41*, 2385.
(35) Jusys, Z.; Kaiser, J.; Behm, R. J. *Electrochim. Acta* **2002**, *47*, 3693.
(36) Tripkovic, A. V.; Popovic, K. D.; Grgur, B. N.; Blizanac, B.; Ross, P. N.; Markovic, N. M. *Electrochim. Acta* **2002**, *47*, 3707.
(37) Shin, J.; Korzeniewski, C. *J. Phys. Chem. B* **1995**, *99*, 3419.
(38) Bruckenstein, R. R.; Gadde, J. *J. Am. Chem. Soc.* **1971**, *93*, 793.
(39) Wolter, O.; Heitbaum, J. *Ber. Bunsen-Ges.* **1984**, *88*, 2.
(40) Wolter, O.; Heitbaum, J. *Ber. Bunsen-Ges.* **1984**, *88*, 6.
(41) Hartung, T.; Baltruschat, H. *Langmuir* **1990**, *6*, 953.
(42) Baltruschat, H.; Schmiemann, U. *Ber. Bunsen-Ges.* **1993**, *97*, 452.
(43) Baltruschat, H. *J. Am. Soc. Mass Spectrom.* **2004**, *15*, 1693.
(44) Jusys, Z.; Massong, H.; Baltruschat, H. *J. Electrochem. Soc.* **1999**, *146*, 1093.
(45) Kita, H.; Lei, H.-W. *J. Electroanal. Chem.* **1995**, *388*, 167.
(46) Jambunathan, K.; Hillier, A. C. *J. Electrochem. Soc.* **2003**, *150*, E312.
(47) Jambunathan, K.; Jayaraman, S.; Hillier, A. C. *Langmuir* **2004**, *20*, 1856.
(48) Wonders, A. H.; Housmans, T. H. M.; Rosca, V.; Koper, M. T. M. *J. Appl. Electrochem.*, submitted for publication, 2005.
(49) Korzeniewski, C.; Childers, C. L. *J. Phys. Chem. B* **1998**, *102*, 489.
(50) Childers, C. L.; Huang, H.; Korzeniewski, C. *Langmuir* **1999**, *15*, 786.
(51) Guthrie, J. P. *Can. J. Chem.* **1975**, *53*, 898.
(52) Winkelman, J. G. M.; Voorwinde, O. K.; Ottens, M.; Beenackers, A. A. C. M.; Janssen, L. P. B. M. *Chem. Eng. Sci.* **2002**, *57*, 4067.
(53) Sun, S.-G.; Lu, G.-Q.; Tian, Z.-W. *J. Electroanal. Chem.* **1995**, *393*, 97.
(54) Miki, A.; Ye, S.; Senzaki, T.; Osawa, M. *J. Electroanal. Chem.* **2004**, *563*, 23.

(55) Chen, Y. X.; Miki, A.; Ye, S.; Sakai, H.; Osawa, M. *J. Am. Chem. Soc.* **2003**, *125*, 3680.
(56) Miki, A.; Ye, S.; Osawa, M. *Chem. Commun.* **2002**, 1500.
(57) Clavilier, J.; Armand, D.; Sun, S. G.; Petit, M. *J. Electroanal. Chem.* **1986**, *205*, 267.
(58) Lebedeva, N. P.; Koper, M. T. M.; Feliu, J. M.; van Santen, R. A. *Electrochem. Commun.* **2000**, *2*, 487.
(59) Al-Akl, A.; Attard, G. A.; Price, R.; Timothy, B. *J. Electroanal. Chem.* **1999**, *467*, 60.
(60) Funtikov, A. M.; Stimming, U.; Vogel, R. *J. Electroanal. Chem.* **1997**, *428*, 147.
(61) Koper, M. T. M.; Lukkien, J. J. *J. Electroanal. Chem.* **2000**, *485*, 161.
(62) Clavilier, J.; El Achi, K.; Rodes, A. *J. Electroanal. Chem.* **1989**, *272*, 253.
(63) Clavilier, J.; Rodes, A. *J. Electroanal. Chem.* **1993**, *348*, 247.
(64) Clavilier, J.; El Achi, K.; Petit, M.; Rodes, A.; Zamakhchari, M. A. *J. Electroanal. Chem.* **1990**, *295*, 333.
(65) Clavilier, J.; El Achi, K.; Rodes, A. *Chem. Phys.* **1990**, *141*, 1.
(66) Gao, Y.; Tsuji, H.; Hattori, H.; Kita, H. *J. Electroanal. Chem.* **1994**, *372*, 195.
(67) Xia, X. H.; Iwasita, T.; Ge, F.; Vielstich, W. *Electrochim. Acta* **1996**, *41*, 711.
(68) Markovic, N. M.; Grgur, B. N.; Lucas, C. A.; Ross, P. N. *Surf. Sci.* **1997**, *384*, L805.
(69) Jarvi, T. D.; Sriramulu, S.; Stuve, E. M. *Colloids Surf., A* **1998**, *134*, 145.
(70) Olivi, P.; Bulhoes, L. O. S.; Leger, J. M.; Hahn, F.; Beden, B.; Lamy, C. *Electrochim. Acta* **1996**, *41*, 927.
(71) Franaszczuk, K.; Herrero, E.; Zelenay, P.; Wieckowski, A.; Wang, J.; Masel, R. I. *J. Phys. Chem. B* **1992**, *96*, 8509.
(72) Iwasita, T.; Vielstich, W.; Santos, E. *J. Electroanal. Chem.* **1987**, *229*, 367.
(73) Willsau, J.; Heitbaum, J. *Electrochim. Acta* **1986**, *31*, 943.
(74) Willsau, J.; Heitbaum, J. J. *Electroanal. Chem. Interfacial Electrochem.* **1985**, *185*, 181.
(75) Vielstich, W.; Christensen, P. A.; Weeks, S. A.; Hamnett, A. *J. Electroanal. Chem. Interfacial Electrochem.* **1988**, *242*, 327.
(76) Wilhelm, S.; Vielstich, W.; Buschmann, H. W.; Iwasita, T. *J. Electroanal. Chem. Interfacial Electrochem.* **1987**, *229*, 377.
(77) Beden, B.; Lamy, C.; Bewick, A.; Kunimatsu, K. *J. Electroanal. Chem. Interfacial Electrochem.* **1981**, *121*, 343.
(78) Davis, J. L.; Barteau, M. A. *Surf. Sci.* **1987**, *187*, 387.
(79) Kizhakevariam, N.; Stuve, E. M. *Surf. Sci.* **1993**, *286*, 246.
(80) Wang, J.; Masel, R. I. *Surf. Sci.* **1991**, *243*, 199.
(81) Wang, J.; Masel, R. I. *J. Vac. Sci. Technol., A* **1991**, *9*, 1879.
(82) Sexton, B. A. *Surf. Sci.* **1981**, *102*, 271.
(83) Olivi, P.; Bulhoes, L. O. S.; Leger, J. M.; Hahn, F.; Beden, B.; Lamy, C. *J. Electroanal. Chem.* **1994**, *370*, 241.